

Iranian Journal of Oil & Gas Science and Technology, Vol. 11 (2022), No. 3, pp. 01–22
<http://ijogst.put.ac.ir>

Casing Selection Strategy to Overcome Buckling Generation and Influences on Cement Quality in Vertical Wells

Abdeslem Leksir*

Ph.D., Instructor, University of Badji Mokhtar Annaba (UBMA), Boukarma, Algeria.

Highlights

- Buckling generation during column cementing is detailed;
- Buckling while testing the critical parameters of the column is proposed;
- Influences of buckling on the cement behind casing quality and cracking of previous column cement are all investigated;
- Casing elongation, Von Mises theories, and a new characteristics selection strategy are directed to indicate the merit of the proposed method.

Received: April 17, 2022; revised: July 07, 2022; accepted: July 20, 2022

Abstract

Column final tests face new challenges, and in addition to casing burst/collapse limitations, buckling occurrence creates serious problems. In case of a slight gap between mud and slurry densities, buckling initiation is inevitable. Casing elongation, bending, and buckling are detailed to define column behavior while testing. Buckling influences on slurry are mentioned and compared to the column without test. A new cement quality indicator is also proposed, tested, and validated via logging of wells drilled in different regions. The results are generalized to cover other situations rather than heavy sections. Further, gas migration regions, depleted reservoirs, and weak zones are all examined. Registrations confirm the appearance of buckling either while pumping slurry or pressure testing. A new modified casing selection method conjointly with an updated numerical technique is proposed to prevent buckling. Moreover, the experimental and simulation findings confirm the reliability of the proposed technique.

Keywords: Casing Buckling, Casing Design and Testing, Cement Quality

How to cite this article

Leksir L, *Casing Selection Strategy to Overcome Buckling Generation and Influences on Cement Quality in Vertical Wells*, *Niger Delta. Iran J. Oil Gas Sci. Technol.*, Vol. 11, No. 3, p. 1–22, 2022.

DOI: [10.22050/ijogst.2022.337958.1636](https://doi.org/10.22050/ijogst.2022.337958.1636)

1. Introduction

To reach the pay zone, drilling wells pass through different sections, and each is sealed off to permit further drilling. Casing running, cementing, and testing represent the success keys of the sealing mechanism (Richard et al., 2014; Kiran et al., 2014; Mohammed et al., 2019).

In addition to handling conventional drilling issues, casing with drilling presents an enormous reduction of nonproductive time (NPT). Several casing phenomena occur, such as Euler elongation (API, 1998), buckling, ballooning, piston effects, and temperature variations (William et al., 2016). The interaction

* Corresponding author:

Email: leksir1@yahoo.fr

of numerous phenomena during cementing makes distinguishing the real cause of failure hard. Flash setting (Javed, 1987), incorrect setting (Choudhary et al., 2015), downhole mechanical problem (Thomas et al., 2015; Clark, 1987), and formation restriction present practically the same characteristics. A new method was presented by Leksir (2020a) to differentiate pressure increase due to chemical reactions named flash setting from other probable problems. Leksir (2020b) presented the phenomenon of casing elongation during heavy slurry displacement inside the casing due to the high frictional force exerted, which requires extra surface pressure. Jiwei et al. (2019) reported the influences of a casing pressure test on cement seal integrity. Klinkenberg (1951) and Lubinski (1962) demonstrated the influences of fluid characteristics on neutral point position and buckling generation based on *fictitious* force analysis. Later, Hammerlindl (1980) generalized fluid influences theory on string tensile force to cover different pressures and densities. More oriented papers (Chen et al., 1990; Mitchell, 1999) have presented an applied method to analyze the buckling effect on deviated wells, referred to as “Paslay force”. Other studies that focus on completion systems or oriented toward horizontal wells are presented in Table 1.

Table 1
Casing buckling.

Buckling system	References
Completion	Yinping et al., 2017; Mitchell, 1986; De-Li and Wen-Jun, 2015; Gao et al., 1998.
Horizontal wells	Dawson and Paslay, 1985; Barakat et al., 2007; Daily et al., 2013; Dellinger, 1983; Gao and Miska, 2009; Gao and Miska, 2010a.

Buckling is generated once equivalent hydrostatic pressure inside the column overcomes the outside casing (Clark, 1987). In vertical wells, buckling occurs at relatively low compressive force compared to horizontal, and depending on the compression degree, the state change from sinusoidal to helical (Jellison and Brock, 2000). Moreover, Mitchell (2004) specified that when a static-constrained column was exposed to an axial, compressive-force-induced torque generated may exceed tubular makeup torque due to helical buckling.

The paper presents the phenomenon of casing buckling arising while testing the column. If equivalent inside and outside casing densities are almost similar at the end of cement displacement, compressive force initiated, additional weight recovered, and consequent elongation due to buoyancy change is sufficient to tag the bottom; thus, the casing will have particular behavior while testing (Jellison and Brock, 2000). Surface pressure will rapidly push inside equivalent pressure to overcome the outside one. Moreover, additional force is generated due to the reduction in the buoyancy effect (Arnfinn and Naval, 2017). Buoyancy force receives vast variations, and equivalent hydrostatic pressure rapidly varies while pumping fluids from inside to outside casing, compared to the initial homogeneous conventional system. More specifications concerning buoyancy changes are presented elsewhere (Eirik, 2011; Arnfinn and Naval, 2017).

Knowing that the space between the casing and total depth is limited, the additional force will engender supplementary casing elongation and may lead to touching the bottom hole (Clark, 1987).

2. Cement job and buckling generation

Cement job is the operation that guarantees the efficiency of the sealing system and preserves the integrity of the well (De Andrade et al., 2016; Catalin et al., 2013) via mud removal and good slurry placement technics (Pelipenko and Frigaard, 2004; Kevin et al. 2019). In order to repair primary-

cementing problems, high-cost and complicated techniques are required with a low possibility of success. Oil well cement is primarily selected as class G or H depending on the range of well depth, temperature, and pressure. At the end of the operation, a pressure test must run to detect any leak-off (Jiwei et al., 2019). In conventional column architecture, slurry density is much higher than drilling fluid, which may influence equivalent circulation density (ECD: sum of static hydrostatic pressure with friction pressure) rather than a static state. In order to achieve the equilibrium state while testing, high pressure should exert from the surface. In a nonconventional system (heavy slurry and depleted reservoir) where the difference in equivalent hydrostatic pressure from inside to outside is valueless, the surface pressure needed to reach equilibrium is remarkably low. Consequently, the positive action of equivalent internal forces initiates, and phenomena of casing elongation are induced (Leksir, 2020b).

Before the beginning of the casing test, influenced by slurry density behind the casing, the column receives a reverse ballooning effect (Akgun, 1996). Generally, a conventional system needs further inside surface pressure to overcome reverse ballooning. At this moment, the column recovers additional weight and becomes longer. Consequently, the casing may tag the bottom, which induces compressive force and buckling.

Figure 1 presents an open-hole caliper compared to cement bond evaluation logs. The open hole is straight and gagged, without remarkable washout or restriction. I-SCAN ultrasonic logging confirms the low-quality cement obtained via sonic log, and I-SCAN shows a helically shaped form, especially in the VDL part. Initially, this phenomenon is interpreted as liquid material behind the casing, considering that the upper part presents good bond cement, and the helical form still appears.

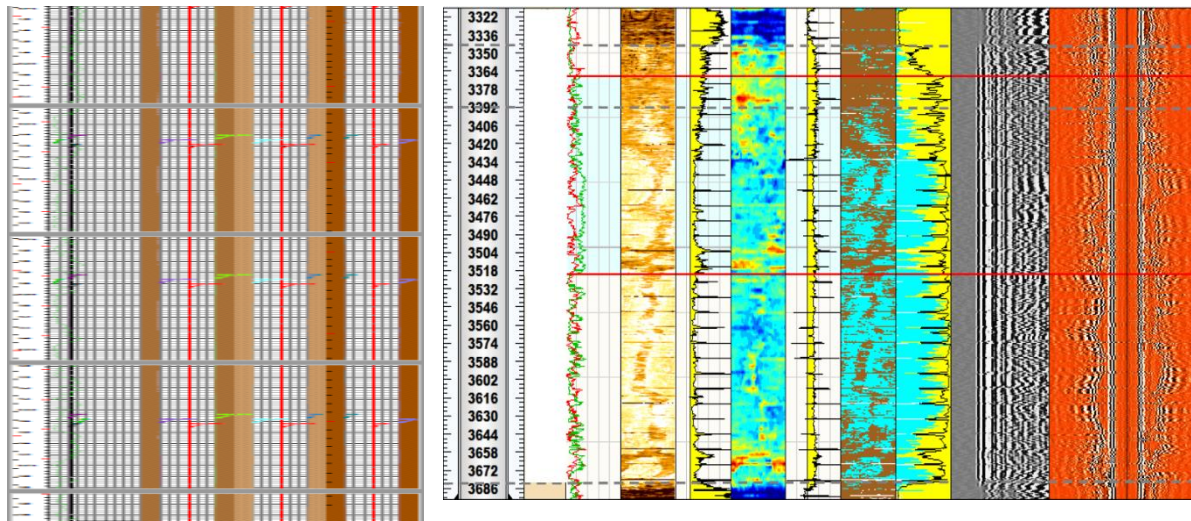


Figure 1

Open hole logging (caliper) and cement bond evaluation.

Via the utilization of the casing elongation theory detailed by Leksir (2020b), the same considerations will be applied to column testing. Equation (1) expresses the casing elongation equation:

$$E = (F_a - (A_o P_o - A_i P_i)) * (L) / (735294 * w) \quad (1)$$

Table 2 lists the well characteristics. Introducing well specifications presented in Table 2 in relation to Equation (1), we can present the results in Table 3.

Table 2

Well specifications.

Well specification (Unit)	Value
TD (m)	3698
Mud density (sg)	2,20
Slurry density (sg)	2,24
Casing (in)	9" 5/8
Column pressure test (psi)	3500

Table 3

Casing elongation.

Casing elongation	(in)	(m)	[(EWT/EWOT)-EWHM] (m)
Elongation without test (EWOT)	153,22	3,9	-0,0506
Elongation with test (3500 psi) (EWT)	225,87	5,74	1,7947
Elongation with homogeneous mud (EWH)	155,21	3,94	/

In Table 3, the casing emergences in homogeneous mud gain an elongation of 3.94 m. Conversely, as cement is placed in the annulus, the casing receives a shortage of 0.05 m. Raising surface pressure to 3500 psi produces an elongation of around 1.8 m, knowing that space-out CSG-TD is limited, exceeding this boundary buckling initiate.

This phenomenon may appear as low-quality bond cement when cementing through the dead formation. Inversely, when gas, water, weak formation, or any other geological layer with specific characteristics that could generate inflow/outflow of fluids is present, a critical situation may occur. Moreover, even in dead formations, if cement loses part of its water caused by direct contact with the formation, the flash setting could occur during displacement (Catalin et al., 2013).

Casing buckling force is given by Lubinski (1962) as follows:

$$F_b = F_a + A_i P_i - A_o P_o \quad (2)$$

where F_b is the buckling force (lbf), and F_a indicates the casing tension force (lbf).

F_b is the sum of unvarying forces (F_a) generated by casing weight and additional variable force ($A_i P_i - A_o P_o$) related to downhole conditions, where A_i is the area of the casing's internal diameter (in²), A_o represents the area of the casing's outer diameter (in²), P_i denotes the equivalent inside casing bottom pressure (psi), and P_o is the equivalent annulus bottom pressure (psi).

Generally, the suspended casing is exposed to tension force generated by the column weight. Fluid density and flow rate variations will influence the total weight suspended (Leksir, 2020b). Elongation due to tension load is given by the following (API, 1998):

$$E = (L * T) / (735000 * W) \quad (3)$$

where E is the tension load elongation (in), T indicates the tension load (lb), and W represents the buoyed weight per unit length (lbf/in) defined by Lubinski (1962) as $W = W_s + W_i - W_o$; W_s indicates

the weight of steel per unit length (lbf/in), W_i is the weight of fluid inside the casing per unit length (lbf/in), and W_o is the fluid weight outside the casing per unit length (lbf/in).

As casing tags, the bottom compressive force (F_{cr}) initiates, and buckling equation will be given by the following:

$$F_{Nb} = F_b - F_{cr} \quad (4)$$

where F_{Nb} is the new buckling force. The rise of compressive force (F_{cr}) pushes the casing to bend until it touches the wellbore.

3. Model of casing buckling in vertical wells

Critical buckling load is the key to casing design in the vertical section. Leksir (2020b) presents a new point of view to define the beginning of buckling during cementing. Displacing heavy slurry inside the casing could lead to overcoming outside equivalent behavior ($A_o P_o$) by the inside ($A_i P_i$). More precisely, the additional force generated ($A_i P_i - A_o P_o$) is remarkably lower than a conventional homogenous system $(A_i - A_o) P_h$. Consequently, more column weight is recovered, and additional casing elongation is engendered. Even if the outside equivalent hydrostatic pressure is slightly higher than the inside, high-pressure testing may cause elongation sufficient to close the bottom passage (CSG-TD). Higher testing pressure means the situation tends to pass from simple bending to a helical shape. In vertical wellbore, the main characteristics of buckling are compressive force, helix pitch, and contact force.

The contact force (F_N) acted toward wellbore is given by Equation (5) (De-Li and Wen-Jun, 2015):

$$F_N = (F_{cr}^2 r) / (4EI) \quad (5)$$

Before tagging the bottom, compressive force $F_{cr} = 0$, the contact force is valueless. When the casing column elongates and touches the bottom, $F_{cr} \neq 0$ and $F_N \neq 0$.

As the compressive force increases, the straight column converts to a helically shaped structure; helix pitch P is calculated as follows (Lubinski, 1962):

$$P = \sqrt{8\pi^2 EI / F_{cr}} \quad (6)$$

In Equation (6), the helix pitch value decreases when compressive force increases, indicating that the number of helix circles rises, and the column tends to compact. Keep increasing pressure leads to generating a more compressive force.

Dawson and Paslay (1985) proposed a minimum buckling force named ‘‘Paslay force’’, as given in Equation (7):

$$F_p = 2 \sqrt{(EIW * \sin \varphi) / r} \quad (7)$$

where r is the casing-to-open hole radial clearance (in), and φ indicates the inclination angle from the vertical.

In vertical wells, the inclination angle is equal to zero. Consequently, $F_p = 0$, and helical buckling of the column will initiate any compressive force exerted from the bottom (Economides, Michael et al., 1998). Inversely, in inclined wells, a significant part of the casing lies on the wellbore; inducing buckling needs more force (Economides, Michael et al., 1998).

Lubinski (1962) proposed an analytical method to calculate the required parameters, supported by casing, before reaching permanent corkscrewing. Column buckling could damage formation and casing

downhole equipment (Lubinski, 1962) and may influence cement quality. Even if the casing returns to its initial state, geological formation, and slurry will not have the same behavior.

The primary measure that must be verified to avoid casing yielding is given by the maximum distortion energy theory (Andre et al. 2020). Von Mises criterion analysis of plastic failure in metals is given by the following:

$$S_x = 1/\sqrt{2} \sqrt{(\delta_t - \delta_r)^2 + (\delta_r - \delta_z)^2 + (\delta_z - \delta_t)^2} < S \quad (8)$$

where S_x indicates the von Mises stress, δ_t and δ_r are the tangential and radial stress, respectively, δ_z represents axial stress, and S is yield strength. Lubinski (1962) simplified Equation (8) for buckling investigation. The formulas for both inside and outside stress verifications induced by pressure variations are given by the following:

$$S_o = \sqrt{3[(P_i - P_o)/(R^2 - 1)]^2 + [(P_i - R^2 P_o)/(R^2 - 1) + \sigma_a \mp \sigma_b]^2} \leq S \quad (9)$$

$$S_i = \sqrt{3[(R^2(P_i - P_o))/(R^2 - 1)]^2 + [(P_i - R^2 P_o)/(R^2 - 1) + \sigma_a \mp \sigma_b/R]^2} \leq S \quad (10)$$

where P_i is inside equivalent pressure, P_o indicates outside equivalent pressure, R represents the casing ratio defined as OD/ID, $\sigma_b = Dr(F_{cr}/(4I))$, $\sigma_a = F_c/A_{cr}$, $F_c = A_o P_o - A_i P_i$, and A_{cr} denotes the cross-sectional area of the casing wall.

At any point in the casing column, the principal stress (S_x) must be less than tensile yield strength. This work refers to minimum yield strength rather than tensile strength to minimize casing damage interval.

3.1. Problem description

Figure 2 illustrates the difference between conventional and heavy slurry. In conventional slurry, casing elongation will not touch the bottom, even when surface pressure reaches a high level (3500 psi). Conversely, elongation in a heavy slurry column will reach the bottom at only 2000 psi. Buckling initiates at this instant, and raising pressure will worsen the situation. Figure 2 shows different casing weights (W) elongation while testing. Using conventional slurry (1.9 sg), the pressure needed to elongate the casing to tag the bottom is around 3000 psi.

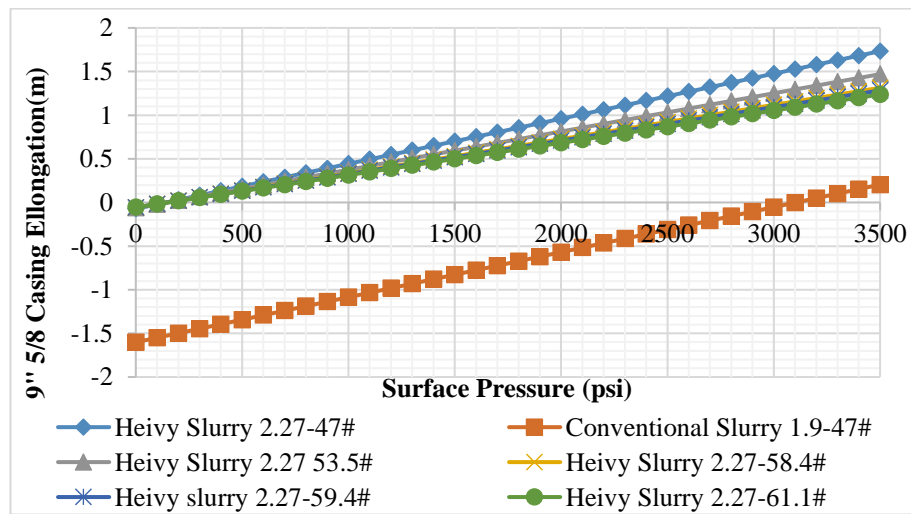


Figure 2

Casing elongation during the final column test for conventional and heavy slurries.

The phenomenon of buckling during heavy slurry column testing is presented in the below sequences:

1. Casing before testing (safe position);
2. Elongation and touch the bottom (buckling);
3. Column bending (bending);
4. Contact between column and well bore (sinusoidal);
5. More force is exerted, and a helical shape is generated (helical).

Figure 3 presents the influences of surface pressure on compressive force. Low casing weight (W) will generate more force; inversely, high casing (W) only generates force at high testing pressure.

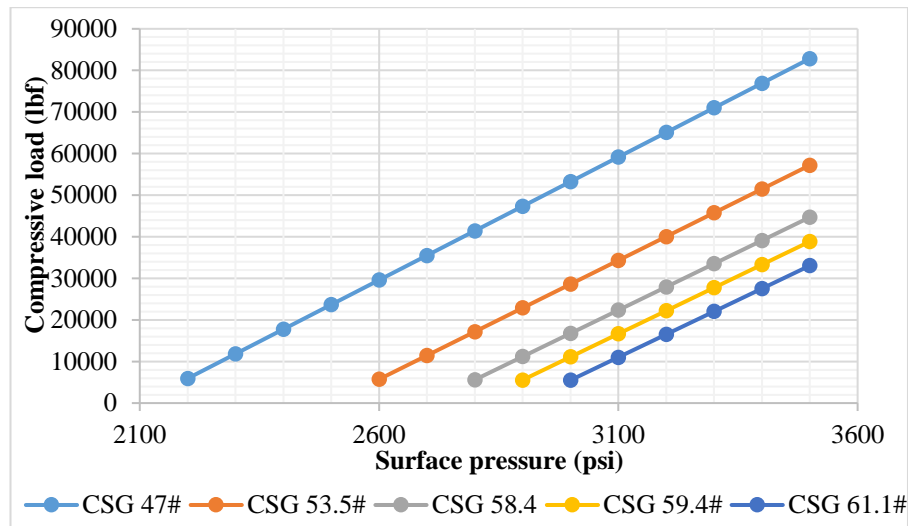


Figure 3

The compressive force generated while rising surface pressure.

The column progressively bends until it makes contact with the wellbore. The overall casing form modifies, and corkscrewing shape appears. As pressure rises, the number of pitches increases (Figure 4) to reach an irreversible state when the equivalent principal stress equals the tensile yield stress of the casing (Figure 5). If this state is achieved, the pipe will receive permanent deformation.

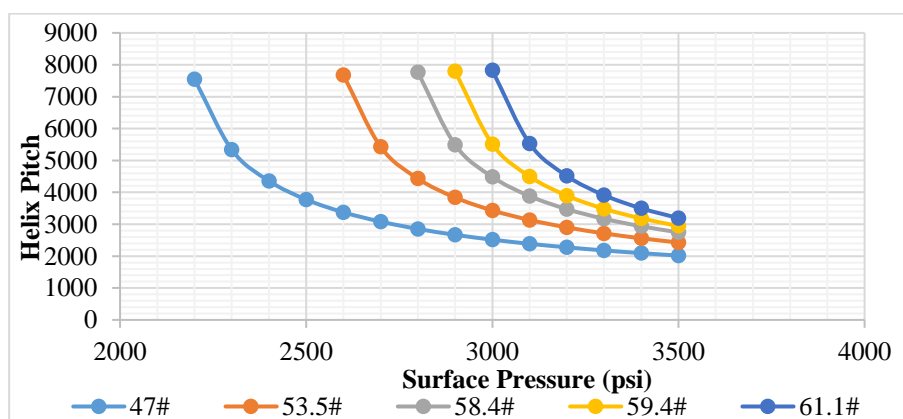
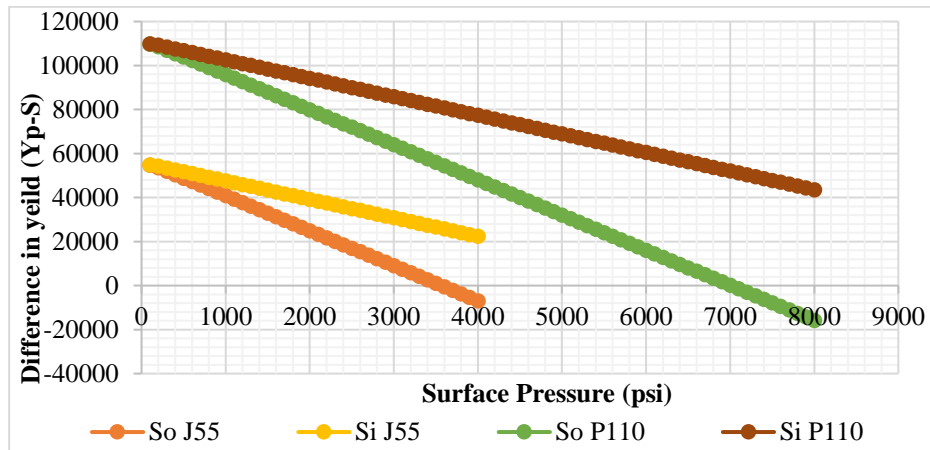


Figure 4

Helix pitch variations while rising surface pressure.

**Figure 5**

Yield strength variation while rising surface pressure.

Figure 5 compares principal stress to the minimum yield, and the risk of damage to the casing occurs when the difference equals zero. Testing at a pressure equivalent to zero weight reduction is stopped if this situation appears.

In order to achieve good bond cement quality, the below parameters should be preserved (see Table 4).

Table 4

The column test parameters while buckling.

Parameters	Description
1 Space out	The gap between CSG and TD ensures fluids circulate.
2 Casing elongation	CSG elongation due to fluid density variation from outside to inside.
3 Touching bottom	Elongation causes the CSG–TD gap to close, suddenly raising SPP.
4 Buckling initiation	As CSG touches the bottom, compressive force generates, and buckling starts.
5 Neutral point position	Neutral point
6 Bending initiation	When the casing loses its verticality.
7 Sinusoidal	Casing buckling initially has a sinusoidal shape.
8 Helical	Continuing rising pressure column will have a helical shape.
9 Contact force	Casing contact force acting on the inside wall of the well.
10 Open hole influences	Formation faced, contacting area affected.
11 Cased hole influences	The influence extends to the cased hole if the neutral point reaches the previous CSG depth.
12 Slurry quality influences	As slurry density is close to mud density, the probability of buckling rises.
13 TD influences	As TD is greater, the difference in hydrostatic will be more significant, and buckling may appear.

Buckling during cement displacement severely affects the smooth running of operations (losses, inside flow plugging, and doubted situations similar to flash setting) (Leksir, 2020b). However, buckling during the column test will directly affect cement quality. Figure 6 shows the placement of heavy slurry in the open hole without any column weight reduction. Differently, while testing the column, a considerable reduction in hook load is registered.



Figure 6

Buckling generation while pressure testing (without weight reduction during placement).

3.2. New characteristics selection strategy

Generally, the section selection length is referred to geological limitations. Variations in formation pressures make drilling a long hole using the same fluid density impractical. In order to overcome this problem, the casing will run, and the cement will seal off the current section and permit further drilling.

Elongation theory: enormous variation in buoyancy force is received while pumping and displacing slurry to the annulus. Column weight changes accordingly, and additional weight may gain. Extra Euler elongation of casing due to additional weight may reach the total depth.

Maximum reachable equivalent hydrostatic pressure is chosen based on the elongation theory. Surface pressure rises, and the casing shape deforms accordingly. This critical situation represents the key to the new casing design process. The casing type and grade will be chosen according to maximum elongation. If the required volume and density are needed to seal off the desired open hole, the elongation theory is verified, and then one slurry type is used. If not, two slurries are required: a conventional tail to keep a consistent shoe and a lightweight one to remain all open hole sealed.

During all displacement sequences, ΔE must be inferior to the space-out length. Hydrostatic pressure must be lower than the formation pressure to avoid losses.

Maximum elongation limitation is given by Equation (11):

$$\Delta E < \Delta L \quad (11)$$

where ΔL indicates space-out CSG–TD.

The other constraint defined as hydrostatic pressure compared to formation fracture is given by the following:

$$H_F \geq H_c + H_m \quad (12)$$

where H_F is the fracture pressure of the formation, H_c represents cement hydrostatic pressure, and H_m indicates hydrostatic mud pressure.

The total length is defined as follows:

$$L = L_c + L_m \quad (13)$$

Knowing that $\Delta L = L - L_0$, L_0 is the total length of the hole, and Equation (10) is expressed by:

$$\Delta E - \Delta L = 0 \quad (14)$$

Knowing that $\Delta E = ((\pi * 0.052)/(735294)) * ((r^2 L^2)/W) * (\rho_i - \rho_o)$ (Leksir, 2020b), Equation (13) is written as follows:

$$((\pi * 0.052)/(735294)) * ((r^2 L^2)/W) * (\rho_i - \rho_o) - \Delta L = 0 \quad (15)$$

Assuming that $\Delta L = 1m$, L_{max} before testing is given by Equation (16):

$$L_{max} = \sqrt{(177293757.84 * W)/(r^2(\rho_i - \rho_o))} \quad (16)$$

In the case of column testing, following the same operations, L_{max} is defined as:

$$L_{max} = \sqrt{177293757.84 * W/(r^2((\rho_{istatic} + \rho_{itest}) - \rho_o))} \quad (17)$$

As the maximum length is fixed geologically, the inside maximum hydrostatic pressure is given by:

$$\text{Knowing that } H_i = 0.052 * L * \rho_i \text{ and } H_o = 0.052 * L * \rho_o \quad (18)$$

Equation (18) is expressed by:

$$(\pi/(735294)) * (r^2 L/W) * (H_i - H_o) = \Delta L \quad (19)$$

Finally, inside hydrostatic pressure is given by:

$$H_i = H_o + [(234170W)/(r^2 L)] \Delta L \quad (20)$$

In order to find the maximum value of hydrostatic pressure before tagging, the bottom ΔL should be equal to space-out CSG-TD.

$$H_{i-max} = H_o + (9219275.41W)/(r^2 L) \quad (21)$$

Maximum hydrostatic pressure is divided into three parts: conventional slurry, lightweight slurry, and the required surface pressure to keep fluids in movement.

$$H_{i-max} = H_{cem} + H_{lightcem} + P_{surf} \quad (22)$$

Surface pressure is selected as the minimum pressure necessary to keep fluids in movement and maintain mud removal efficiency.

Slurries hydrostatic column height is determined to fulfill geological requirements. If conventional slurry use exceeds the formation fracture limit, progressive switching to lightweight is required until the optimum design is reached.

$$\sum_{i=1}^{i=n} H_{lightcem} = H_{Frac} - \left(\sum_{i=1}^{i=N} H_{Cem} + H_{mud} + P_{surf} \right) \quad (23)$$

The optimum is found when the combination of reduction in conventional slurry and addition in lightweight slurry does not exceed fracture limits. This is later presented in Equation (24).

$$H_{Geo Req} \leq H_{i-max} + H_{mud} \leq H_{Frac} \quad (24)$$

As casing and cement properties are selected, the slurry is pumped safely and placed behind the casing. A pressure test should run to confirm column integrity.

The surface testing pressure is selected via the maximum hydrostatic pressure generated before touching the bottom, as presented in Equation (25):

$$H_{max} = H_{Cem} + H_{mud} + \sum_{i=1}^{i=N} P_i \quad (25)$$

Knowing that $P_{surf} = \sum_{i=1}^{i=N} P_i$, surface pressure is increased to reach the elongation limit when $i = N$.

In practice, there is a significant difference in pressure testing distribution throughout the casing length between conventional and heavy slurry systems. The practical testing pressure is exerted from the inside to the outside column. In a conventional slurry system, density is much higher than mud density, and a vast part of surface pressure is consumed to overcome the cement behind the casing U-tube effect during testing. Differently, in heavy slurry systems, hydrostatic pressure differences are practically valueless (see Figure 7).

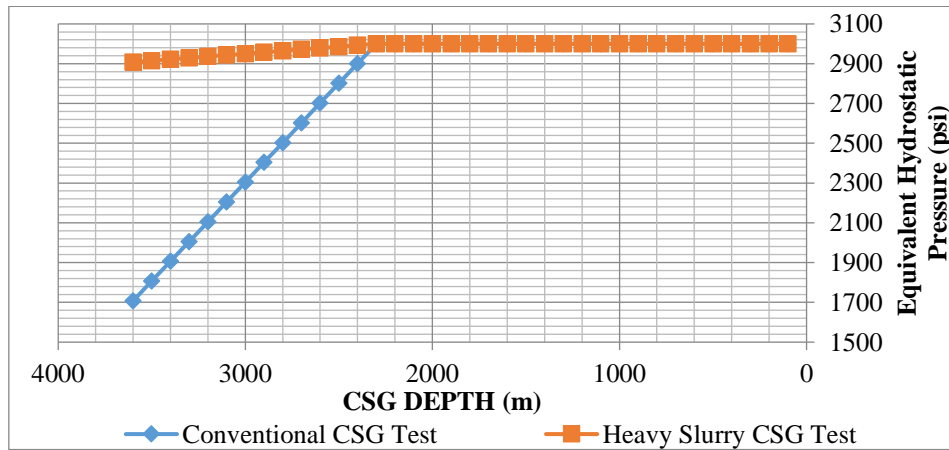


Figure 7

Casing pressure test (3000 psi) of conventional and heavy slurries.

Figure 7 presents the variation in the equivalent hydrostatic pressure of conventional and heavy slurry. Both systems do not receive any variation until reaching the top of the cement. After that, equivalent pressure decreases rapidly to 1700 psi when testing conventional slurry, compared to heavy slurry where pressure is reduced to 2900 psi. This later confirms a large gap between the two processes in effective testing pressure.

4. Cases studies

Some case studies are presented to clarify the feasibility of space-out closing and buckling generation assumption during cement displacement or the column test. More details can be found in Appendix A.

4.1. Heavy slurry

12" 1/4-hole section depth 4000 m, 9"5/8 casing, mud density 2.27 sg. 9"5/8 casing run to TD (total depth) and 13"3/8 previous casing set at 2300m. The total slurry volume anticipated for the seal-off section equals 55.5 m³. The first step in casing design is calculating the maximum inside hydrostatic pressure corresponding to the selected cement volume. Using Equation (17), $H_{i-max} = 14654$. Table 5 presents the value of H_i (47#) corresponding to surface pressure.

Table 5

The correlation of the hydrostatic pressure and maximum length with SPP.

SPP (psi)	100	400	600	800	1000	1200	1700	1900	2000	2300
H_i (psi)	13085	13385	13585	13785	13985	14185	14685	14885	14985	15335
L_{max} (m)	12331	7609	6401	5631	5086	4673	3965	3760	3668	3394

SPP equivalent to 1700 psi guarantees the smooth running of the job. Equivalent hydrostatic pressure will be greater than H_{i-max} , and L_{max} will be smaller than the hole section depth to reach this value; thus, the job will not be completed adequately.

If, according to job simulation and offset wells, the operation running is expected to generate more pressure than H_{i-max} , a new casing weight is selected, as presented in Table 6.

Table 6

The variations of the maximum hydrostatic pressure according to the casing weight.

CSG (#)	47	53.5	58	61.1
H_{i-max} (psi)	14654	14896	15064	15180

Moving from the lower to upper casing weight provides a larger working interval, and SPP rises without influencing the job.

In vertical wells, Paslay force is valueless; consequently, any compressive force generated from the bottom will lead to the column helical (Alexandre, 2016). Table 7 presents the evolution of maximum hydrostatic pressure according to standpipe pressure.

Table 7

The variations of hydrostatic pressure with SPP.

SPP (psi)	500	1000	1500	1800	1900	2000	2500	3000	3500	4000	4500
H_i (psi)	13401	13901	14401	14701	14801	14901	15401	15901	16401	16901	17401

Referring to Equation (17), the maximum allowable hydrostatic pressure for 9"5/8 (47#) casing is $H_{i-max} = 14789$ psi. As a result, testing pressure without buckling generation is limited to 1800 psi.

The maximum hydrostatic pressure is selected via Table 8 if another casing weight is used.

Table 8

Variations of the maximum hydrostatic pressure according to the casing weight.

CSG (#)	47	53.5	58	61.1
H_{i-max} (psi)	14789	15031	15214	15314

4.2. Depleted reservoir and week section

Unlike the conventional section, the depleted reservoir/week section presents low fracture pressure, engendered by excessive production/geological characteristics (Table 9).

Table 9

Week section characteristics.

Hole 12"1/4 (m)	Previous CSG (13" 3/8) Shoe (m)	CSG (47#) 9"5/8 (m)	Mud (sg)	Tail Slurry (Sg)	Lead Slurry (Sg)	estimation Fracture (sg)	TOC (m)
1909	536	1908	1.05	1.90	1.28	1.34	336

Following the identical sequences as heavy slurry, we summarize the variations of inside hydrostatic pressure induced by increasing standpipe pressure in Table 10.

Table 10

The evolution of inside hydrostatic pressure induced by rises of SPP.

SPP (psi)	100	150	200	500	2000
Hi (psi)	3582	3632	3682	3982	5482

Knowing that $H_{i-max} = 6521$ and $H_{frac} = 3634$, the system appears as far from having a casing elongation problem. Differently, losses appear at low SPP, knowing that only the shoe is covered by tail slurry.

Table 11

The variations of hydrostatic pressure with SPP.

SPP psi)	500	1000	1500	2000	2500	3000	3500	3600	3700	4000	4500
Hi (psi)	3348	3848	4348	4848	5348	5848	6348	6448	6548	6848	7348

Even if the simulation results presented in Table 11 show that the high-pressure test is far from generating buckling till around 4500 psi ($H_{i-max} = 7211$), actual results demonstrate a reduction in column weight during testing at 3000 psi. In all cases presented in this paper, space-out CSG–TD is assumed to be 1 m. If the interval is smaller, all characteristics must be recalculated, and an indication of the problem appears earlier.

5. Buckling force calculation

The value of the additional force mentioned in Equation (1) is reduced during the column test. If hydrostatic pressure rises sufficiently to overcome the outside, casing elongation may close the hole space-out. Equation (26) expresses the maximum compressive force supported by the column before buckling initiation.

$$F_{bmax} = (735294 * W/L) * \Delta L \quad (26)$$

where ΔL is the space-out between the casing and total depth (in).

In order to check the buckling, either during displacement or during testing, F_{bmax} must be compared to the instantaneous force presented in Equation (27).

$$F_{bi} = A_i(P_{hi} - P_h) - A_o(P_{ho} - P_h) \quad (27)$$

where P_{hi} indicates inside equivalent hydrostatic pressure during slurry displacement (psi), P_h is homogeneous mud hydrostatic pressure (psi), and P_{ho} represents outside hydrostatic pressure (psi).

Generalizing Equation (27) is employed to calculate buckling force. During displacement inside the casing, ($P_{ho} = P_h$) is presented as:

$$F_{bi} = A_i(P_{hi} - P_h) \quad (28)$$

However, during the column testing, inside hydrostatic is equal to surface pressure ($P_{hi} - P_h = P_{hsurf}$), and outside variation is equal to slurry column hydrostatic pressure ($P_{ho} - P_h = P_{hcem}$). Buckling force generated while testing is presented below:

$$F_{bi} = A_i(P_{hsurf}) - A_o(\Delta P_{hcem-mud}) \quad (29)$$

where $\Delta P_{hcem-mud}$ is the change in hydrostatic pressure between cement and the mud column.

Equation (30) expresses the risk interval and the safe zone.

$$F_{bi} = \begin{cases} F_{bi} < F_{bmax}, & \text{No buckling} \\ F_{bi} \geq F_{bmax}, & \text{Column buckle} \end{cases} \quad (30)$$

Figure 8 presents ($F_{max} - F_{bi}$) variation during conventional and heavy slurry displacement. Due to the U-tube described by the free fall phenomenon (Wellington and Ademar, 1993), an equilibrium state is continually preserved. Inversely, the heavy system ($F_{max} - F_{bi}$) decreases to reach a negative sign at around 1500 psi, indicating the beginning of buckling.

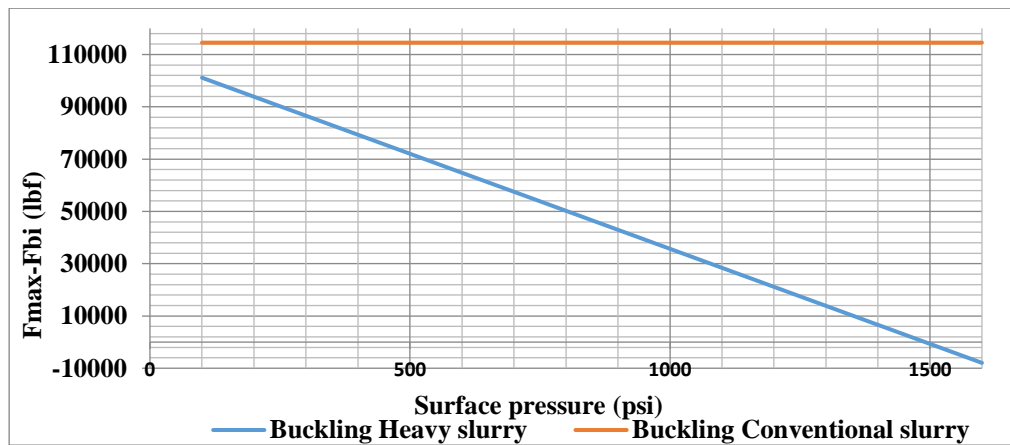


Figure 8

Buckling force variations during conventional and heavy slurry displacement.

In a conventional system (see Figure 9, the blue line), testing pressure rises to 4500 psi without exciting buckling. In the heavy system, where mud and slurry densities are almost equivalent, the buckling state reaches 2200 psi (see Figure 9, the red line).

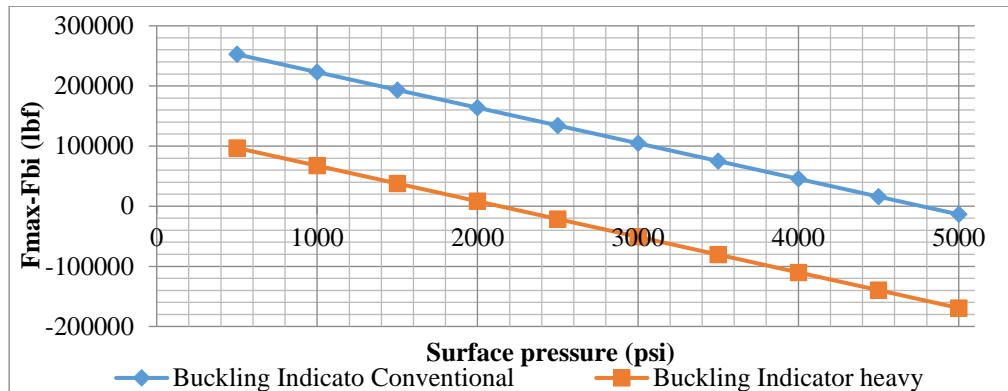


Figure 9

Buckling force variations during conventional and heavy column testing.

In order to overcome buckling occurrences while cementing and testing, two parameters ($F_{max} - F_{bi}$) presented in Figures 8 and 9 should be conserved. These two figures show that casing elongation during conventional cement differs from engender buckling. Inversely, when the slurry is close to the mud density, the ($F_{max} - F_{bi}$) report reaches a negative interval, as shown in Figures 8 and 9, which induces buckling, leading to either interruption of the smooth running of the job or affecting cement behind casing quality. This paper proposes an adequate method for cementing operations and testing without risk generation. Some examples of mud logging charts confirm the bottom tagging while testing and cement quality influences are presented below.

The low quality of the cement bond is the main characteristic of the depleted reservoir and the weak zone log for the column tested at 3500 or 3000 psi (see Figure 10). Conversely, the column tested at 2000 psi presents excellent bond quality (Figure 10).

Casing test/weight reduction Log well 1 test 3500 psi Log well 2 test 3000 psi Log well 3 test 2000 psi

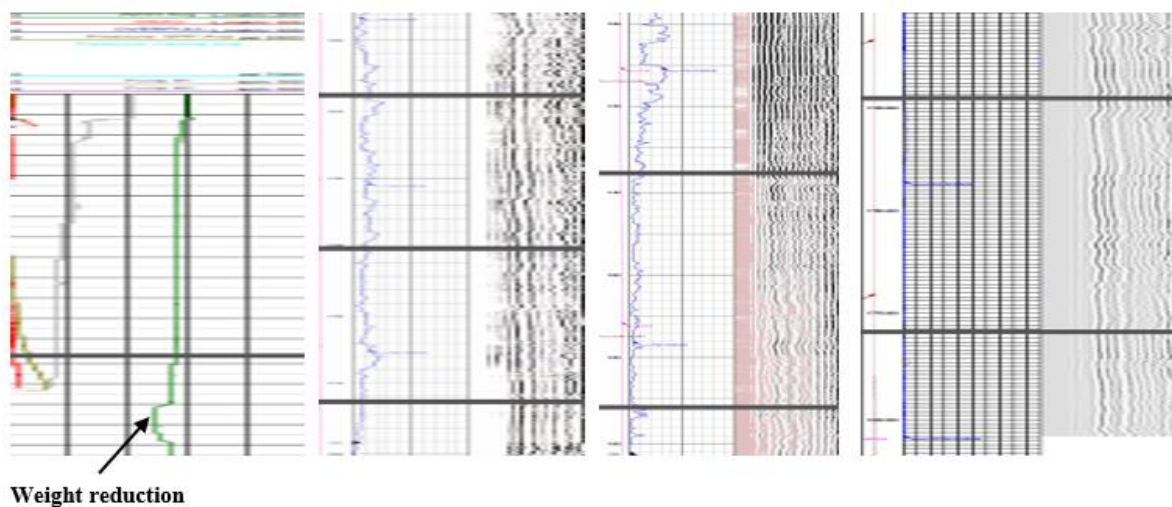
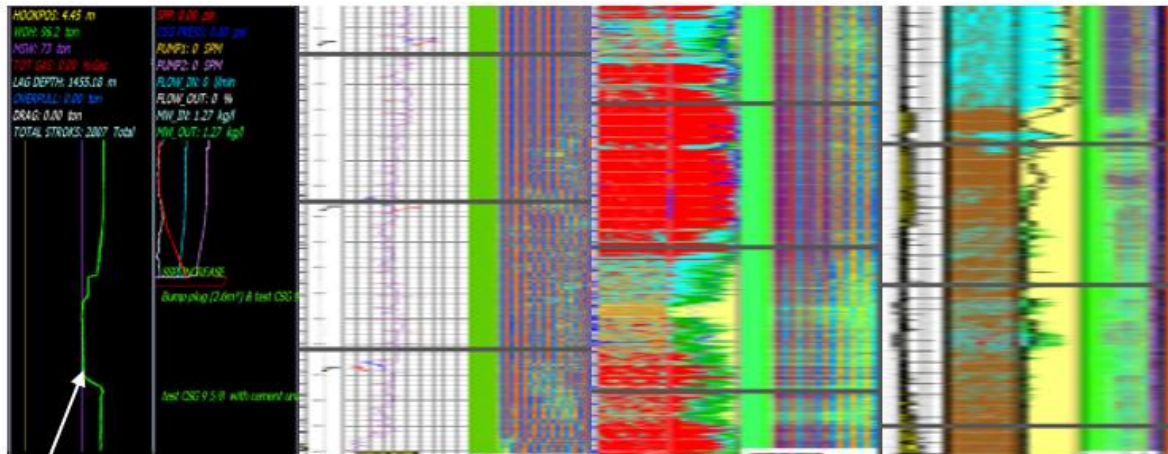


Figure 10

Depleted reservoir, weak zone.

Other phenomena of gas migration appear in some zones where specific characteristics of shallow gas, overpressure region, or shale gas formation are encountered. Figure 11 presents, in addition to weight reduction, motioned in the first column, a series of logging charts for pressure tests 4000 and 3000 psi, where logs show remarkably low-quality cement. The column tested at 2000 psi presents a high-quality cement bond in the last log compared to the previous logs.

Casing test/weight reduction Log well 1 test 4000 psi Log well 2 test 3000 psi Log well 3 test 2000 psi



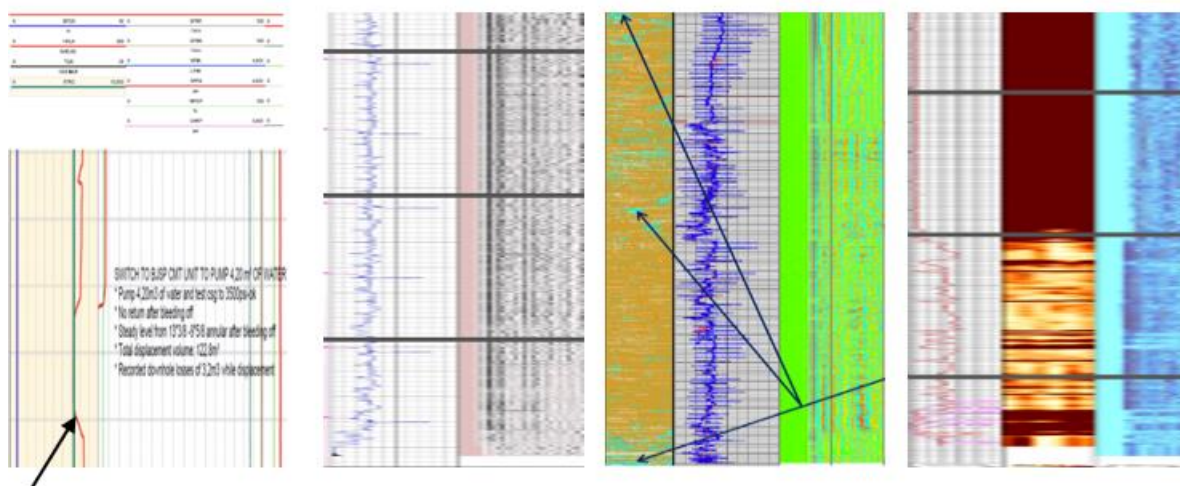
Weight reduction

Figure 11

Logging charts for gas migration zone.

When cementing the heavy section, surface pressure testing may easily support inside hydraulics to overcome the outside one, which engenders column elongation. A low-quality bond is recognized in columns except for the last log, where the column is tested at 2400 psi in Figure 12, showing a series of logs for heavy slurry sections tested at different pressures (3500, 3000, and 2400 psi).

CSG test/ weight reduction Log well 1 test 3500 psi Log well 2 test 3000 psi Log well 3 test 2400 psi



Weight reduction

Figure 12



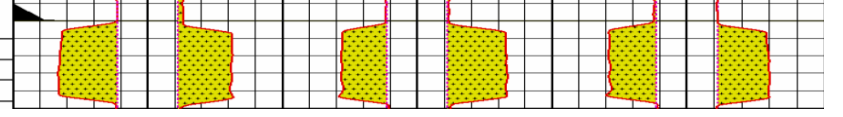
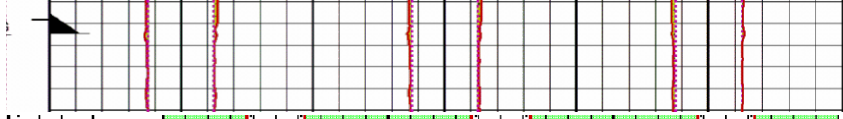
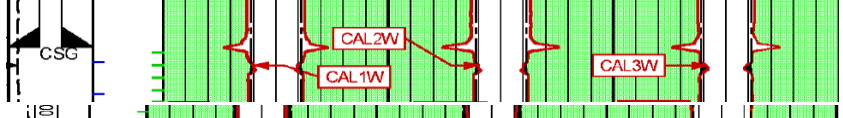
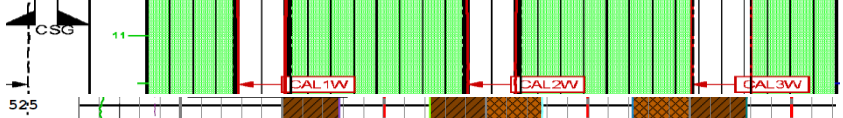
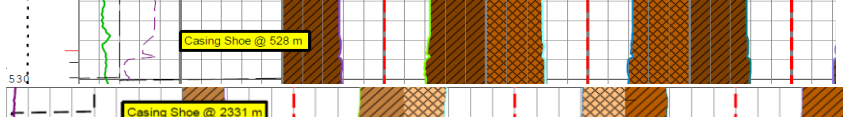

Heavy slurry logging charts.

Knowing that the shoe of the current hole appears in the next section caliper, shoe washout occurring during pressure testing is registered.

Table 12 presents some examples of casing shoes under different pressure conditions.

Table 12

Open hole washout under the shoe under different testing pressures.

Casing/Slurry	Pressure test (psi)	Caliper (log of the following open hole to illustrate the previous section shoe)
18 5/8 (1.9sg)	NO	
13 3/8 (1.35+1.90sg)	4000 psi	
13 3/8 (1.25+1.90sg)	3000psi	
9 5/8 (1.25+1.90sg)	3500psi	
13 3/8 (1.39+1.90sg)	3000psi	
9 5/8 (1.9sg)	3500	
18 5/8 (1.9sg)	NO	
13 3/8 (1.3+1.9sg)	NO	

Columns with no final test (when hydrostatic pressure is vastly greater than inside pressure) have tight shoes compared to columns tested at high pressure. It is worth noting that conventional sonic CBL-VDL detects the quality of conventional cement. A more accurate ultrasonic tool may identify even the helical shape of buckling (Viggen et al., 2020). Other studies could point out buckling influences on the previous casing, geological formation, and downhole equipment.

6. Conclusions

This paper presents the buckling phenomenon of casing during the final test, and the causes and influences are detailed to point out their effects on cement quality. Impacts vary from low-quality cement in dead formations to generating dangerous situations in critical zones.

- Gas migration (sustained casing pressure);
- Weak zone (losses);
- Depleted reservoir (pay zone damages);

- Loss of downhole zonal isolation could be the main feature engendered.

In order to overcome these difficulties, a series of limitations are proposed to prevent buckling.

- Maximum hydrostatic pressure (H_{\max});
- Maximum compressive force supported by the column before buckling initiation ($F_{\max} - F_{bi}$);

These parameters are developed and explored to detect the critical situation before running the casing. The logging results, conjointly with analytical demonstration, approve the credibility of the method exposed and guarantee the efficiency of the solutions proposed.

Nomenclature

A_i	Area of the casing inside diameter (in ²)
A_o	Area of casing outside diameter (in ²)
E	Elongation due to tension load (in)
F_a, T	Casing tension force (lb)
F_b, F_{Nb}	Buckling force (lbf)
F_{cr}	Compressive force (lbf)
F_N	Contact force (lbf)
F_p	Buckling Paslay force (lbf)
H	Hydrostatic pressure (psi)
L	Total column length (ft)
P	Helix pitch number
P_h	Homogenous mud bottom pressure (psi)
P_i	Equivalent inside casing bottom pressure (psi)
P_o	Equivalent annulus bottom pressure (psi)
S_i, S_o	Inside and outside Von Mises stress, respectively
w_i	Inside casing fluid weight per unit length (lbf/in)
w_o	Outside casing fluid weight per unit length (lbf/in)
w_s	Steel weight per unit length (lbf/in)
w	Buoyed weight per unit length (lbf/in)
$\delta_t, \delta_r, \delta_z$	Tangential, radial, and axial stress, respectively
ΔE	Casing effective elongation (in)
ΔL	Space-out CSG–TD (in)

References

- Akgun, F., Rahman, S S., And Kuru, E., Prediction of Microannulus Behind Casings Due to Ballooning Effect: A Key Problem in Gas Wells Australia: N. P., The APPEA Journal, Vol.36 No. 1. p. 575–579. <https://doi.org/10.1071/AJ95035>, 1996.

- Alexandre, L., Effect of Eccentric Annulus, Washouts, and Breakouts on Well Cementing Quality: Laminar Regime Energy Procedia Vol. 86. P. 391–400. <https://doi.org/10.1016/j.egypro.2016.01.040>,2016.
- Andre, T. B., Diogo, L. C., Wellison, J. S. G., Rodolfo, T., Carlos, M. C. J., Empirical Random Kick Model and Casing Reliability" SPE Drilling & Completion, Vol. 35 No. 04. p.644–654. <https://doi.org/10.2118/201200-PA>, 2020.
- API Recommended Practice for Drill Stem Design and Operating Limits, 7G 16th Edition, August 1998.
- Arnfinn, N., Naval, A., The Magic of Buoyancy and Hydrostatics –buoyancy and Effective Forces Modern Applied Science; Vol. 11, No. 12, p 77–83, DOI:10.5539/Mas. Vol.11, No.12, 77 P,2017.
- Barakat, ER., Miska, SZ., Yu, M., The Effect of Hydraulic Vibrations on Initiation of Buckling and Axial Force Transfer for Helically Buckled Pipes at Simulated Horizontal Wellbore Conditions. SPE/IADC Drilling Conference, 20–22 February Amsterdam, <http://dx.doi.org/10.2118/105123-MS>, 2007
- Catalin, T., Christian, K., Mahmood, A., Jerome, S., Arash, S., Wellbore Integrity and Cement Failure at HPHT Conditions, International Journal of Engineering and Applied Sciences, Vol. 2, No.2, 2013.
- Chen, Y. C., Lin, Y. H., and Cheatham, J. B., Tubing and Casing Buckling in Horizontal Wells, J PET Technology, Vol. 42, No. 2., p. 140–191, SPE-1976-PA., <https://doi.org/10.2118/19176-PA>, 1990.
- Choudhary, HK., Anupama, AV., Kumar, R., Panzi, ME., Matteppanavar, S., Baburao, NS., Sahoo, B., Observation of Phase Transformations in Cement During Hydration, Construction, and Building Materials, Vol. 101, Part 1, p. 122–129, <https://doi.org/10.1016/j.conbuildmat.2015.10.027>,2015.
- Clark, HC., Mechanical Design Considerations for Fracture-treating Down Casing Strings, (Includes Associated Papers 17086 and 17124), SPE Drilling Engineering, Vol. 02, No. 2 <https://doi.org/10.2118/14370-PA>,1987.
- Daily, JS., Ring, L., Hajianmaleki, M., Critical Buckling Load Assessment of Drill Strings in Different Wellbores Using The Explicit Finite Element Method SPE Offshore Europe Oil and Gas Conference and Exhibition, Aberdeen, <http://dx.doi.org/10.2118/166592-MS>, 2013.
- Dawson, R., and Paslay, P.R., Drill pipe Buckling in Inclined Holes. J Pet Technol, Vol.36, No. 10, p.1734–1738, <https://doi.org/10.2118/11167-PA>,1985.
- De Andrade, J., Sangesland, S., Skorp, R., Todorovic, J.; Vralstad, T., Experimental Laboratory Setup for Visualization and Quantification of Cement-Sheath Integrity, SPE Drilling & Completion; Vol.31, No. 04. p. 317 – 326, <https://doi.org/10.2118/173871-PA>,2016.
- De-Li, G., Wen-Jun, H. A., Review of Down-Hole Tubular String Buckling in Well Engineering Pet. Sci., Vol. 12, p.443–457, DOI 10.1007/S12182-015-0031-Z,2015.
- Dellinger, T., Gravley, W., Walraven, JE., Preventing Buckling in Drill String, US Patent: p.438-4483, 1983.
- Economides, Michael J., Watters, Larry, T., and Dunn-Norman, Shari, Petroleum Well Construction, John Wiley & Sons, New York, (Chapter 7 (p: 209–214): Casing and Tubing Design – Robert F. Mitchell, Stefan Miska, and Randolph R. Wagner, 1998.

- Eirik Kaarstad, Theory and Application of Buoyancy in Wells Modern Applied Science, Vol. 5, No. 3, June, <https://doi.org/10.2118/101795-MS>, 2011.
- Gao, DL., Liu, FW, Xu BY. An Analysis of Helical Buckling of Long Tubulars in Horizontal Wells SPE International Oil and Gas Conference and Exhibition in China, 2–6 November Beijing, <http://dx.doi.org/10.2118/50931-MS>, 1998.
- Gao, GH., Miska, SZ., Effects of Friction on Post-buckling Behavior and Axial Load Transfer in A Horizontal Well. SPE J., Vol.15, No.4, p.1104–1118, <https://doi.org/10.2118/120084-PA>, 2010a.
- Gao, GH., Miska, SZ., Effects of Boundary Conditions and Friction on Static Buckling of Pipe in A Horizontal Well, SPE J., Vol.14, No.4, p.782–796, <https://doi.org/10.2118/111511-PA>, 2009.
- Hammerlindl, DJ., Basic Fluid Pressure Forces on Oil Well Tubulars, J. Petrol. Technol., Vol. 32, No. 3. p. 153–159, <https://doi.org/10.2118/7594-PA>, 1980.
- Javed, IB., Thermal Monitoring of Flash Setting in Portland Cement Clinkers, Thermochim Acta 199, p.235–241, 1987.
- Jellison, M.J., Brock, J.N., The Impact of Compression Forces on Casing-string Designs and Connectors SPE Drill, & Completion. No. 15, Vol. 4, p. 241–248. <https://doi.org/10.2118/47790-MS>, 2000.
- Jiwei, J., Jun, L., Gonghui, L., Yan, X., and Wai, L., Influence of Casing Pressure Test on Seal Integrity of Cementing First Interface, Trans Tech Publications Ltd, Switzerland. Vol. 944, p 1020–1027, DOI: 10.4028/Www.Scientific.Net/MSF.944.1020, 2019.
- Kevin, N. L., Mtaki ,T. M., Qinggui, W., Haiyang, H., Jun G., Experimental Study on Oil based Mudcake Removal and Enhancement of Shear Bond Strength at Cement-Formation Interface Journal of Petroleum Science and Engineering, Vol. 176, p. 754–761, <https://doi.org/10.1016/J.Petrol.2019.01.066>, 2019.
- Kiran, R., Teodoriu, C., Dadmohammadi, Y., Nygaard, R., Wood, D., Mokhtari, M., Salehi, S., Identification and Evaluation of Well Integrity and Causes of Failure of Well Integrity Barriers (A Review), Journal of Natural Gas Science & Engineering, <https://doi.org/10.1016/J.Jngse.2017.05.009>, 2017.
- Klinkenberg, A., The Neutral Zones in Drill Pipe and Casing and Their Significance in Relation to Buckling and Collapse, Drilling and Production Practice, American Petroleum Institute, p. 64–76, 1951.
- Leksir, A., Maximum Allowable Pressure During Heavy Slurry Displacement, Journal of Petroleum Exploration and Production Technology, Vol. 10, No. 7, p. 2829–2844, DOI: 10.1007/S13202-020-00959-5, 2020b.
- Leksir, A., Oil Well Casing Cement Flash Setting Problem Causes and Identification Strategy based on Cheese Model, Journal of Petroleum Exploration and Production Technology, <https://doi.org/10.1007/S13202-020-00882-9>, 2020a.
- Lubinski, A., Althouse, W.S., and Logan, J.L., Helical Buckling of Tubing Sealed in Packers, SPE Journal of Petroleum Technology, Vol. 14, No. 6, p. 655–670, <https://doi.org/10.2118/178-PA>, 1962.

- Mitchell, R.F., The Twist and Shear of Helically Buckled Pipe SPE Drill Complete, Vol.1, No. 19, p.20–28. <https://doi.org/10.2118/87894-PA>,2004.
- Mitchell, R.F., Simple Frictional Analysis of Helical Buckling of Tubing, SPE Drill Eng, Vol. 1, No. 6., p. 457–465, <https://doi.org/10.2118/13064-PA>,1986.
- Mitchell, R.F., Buckling Analysis in Deviated Wells: A Practical Method, SPE Drill & Compl., Vol. 14, No. 1, p. 11–20, SPE-55039-PA. <https://doi.org/10.2118/55039-PA>,1999.
- Mohammed, A.I., Oyeneyin, B., Atchison, B. and Njuguna, J., Casing Structural Integrity and Failure Modes in A Range of Well Types: A Review, Journal of Natural Gas Science and Engineering [Online], Vol.68, Article ID 102898, <https://doi.org/10.1016/J.Jngse.2019.05.011>,2019.
- Pelipenko, S., and Frigaard, I.A., Mud Removal and Cement Placement During Primary Cementing of An Oil Well Part 2; Steady-state Displacements, Journal of Engineering Mathematics, Vol.48, p.1–26, <https://doi.org/10.1023/B:ENGI.0000009499.63859.F0>,2004.
- Richard, J., Davies, A., Sam Almond, A., Robert, S., Ward, B., Robert, B., Jackson, C. D., Charlotte Adams, A., Fred Worrall, A., Liam, G., Herringshaw, Jon G., Gluyas, A., Mark, A., Whitehead Oil and Gas Wells and Their Integrity: Implications for Shale and Unconventional Resource Exploitation Marine and Petroleum Geology. <http://dx.doi.org/10.1016/J.Marpetgeo.2014.03.001>, 2014.
- Thomas, JJ., James, S., Ortego, JA., Musso, S., Auzerais, F., Fundamental Investigation of The Chemical and Mechanical Properties of High-temperature-cured Oil Well Cements, Offshore Technology Conference, 30 April–3 May, Houston, Texas, USA.,<https://doi.org/10.4043/23668-MS>, 2012.
- Viggen, E.M., Merciu, I.A., Løvstakken, L., Måsøy, S.E., Automatic Interpretation of Cement Evaluation Logs from Cased Boreholes Using Supervised Deep Neural Networks, Journal of Petroleum Science and Engineering, Vol.195, p107-539, 2020.
- Wellington, C., and Ademar Pogglo, Jr, Free-Fall-Effect Calculation Ensures Better Cement-operation Design, SPE Drilling & Completion, p.175–178, September, DOI: 10.2118/21107-PA, 1993.
- William C., Gary, J. P., Michael, D. L., Standard Handbook of Petroleum and Natural Gas Engineering. Third Edition, (Chapter 4), Drilling and Well Completions, Elsevier, p. 414–584, 2016.
- Yinping Cao, Hui Xia, and Yihua Dou Strength Analysis of Helical Buckling Tubing Using Spring Theory Green Energy and Sustainable Development I, AIP Conf. Proc., Vol.1864, p.020163-1–020163-7; <https://doi.org/10.1063/1.4992980>,2017.

Appendix A

Table casing tops, pressure tests, and max compression force (MCF) vs. space out.

Zone	Well No	Mud density (SG)	Previous SG/TOP Liner	Total Td (m)	Casing/Test (psi)	Testing Compressive Force	Max compression force vs. space out				
							0.2m (7.87")	0.4m (15.75")	0.6m (23.62")	0.8m (31.5")	1m (39.37")
Liner	1	1,45	2677	3481	7" (3500)	82261	16220	32440	48660	64880	81101
	2	1,45	2569	3341	7" (3000)	7297	16899	33799	50699	67599	84499
	3	1,45	2648	3475	7" (No test)	-20338	16248	32496	48744	64992	81241
Heavy	1	2,15	2369	3301	9" 5/8 (3500)	204162	25122	50244	75367	100489	125612
	2	2,1	2347	3259	9" 5/8 (3000)	104276	25446	50892	76338	101784	127231
	3	2,04	2367	3311	9" 5/8 (2400)	60361	25046	50093	75139	100186	125233
	4	2,07	2381	3336	9" 5/8 (NO test)	-79608	24858	49717	74576	99435	124294
Week zone (two columns)	1	1	563	1794	9" 5/8 (3500)	132829	46225	92451	138677	184903	231129
	2	1,05	536	1908	9" 5/8 (3000)	101837	43463	86927	130391	173855	217319
	3	1,06	536	1811	9" 5/8 (2000)	49344	45791	91583	137375	183167	228959
Week zone (two columns)	1	1,27	796	1454	9" 5/8 (4000)	201855	57035	114070	171105	228140	285176
	2	1,17	249	1319	13" 3/8 (2000)	-20596	90964	181929	272894	363858	454824
	3	1,2	349	1322	9 5/8 (3000)	119013	62730	125460	188190	250920	313650



This article is an open-access article distributed under the terms and conditions of the Creative Commons Attribution 4.0 International (CC BY 4.0) (<https://creativecommons.org/licenses/by/4.0/>)